ŽILINSKÁ UNIVERZITA V ŽILINE
Strojnícka
fakulta

AUTOREFERÁT
DIZERTAČNEJ PRÁCE

Žilina, 2026 Ing. Dominik Krišák

ŽILINSKÁ UNIVERZITA V ŽILINE
Strojnícka
fakulta

Ing. Dominik Krišák

AUTOREFERÁT DIZERTAČNEJ PRÁCE

Research on Lattice Structures for Additive Manufacturing of Polymers and Metals

Na získanie akademického titulu **d o k t o r**
(„philosophiae doctor", v skratke „PhD.")
v študijnom odbore Strojárstvo
v študijnom programe Automatizované výrobné systémy

Žilina 2026

Dizertačná práca bola vypracovaná v dennej forme doktorandského štúdia na Žilinskej univerzite v Žiline, Strojníckej fakulte, Katedre obrábania a výrobnej techniky.

Predkladateľ: Ing. Dominik Krišák
Žilinská univerzita v Žiline
Strojnícka fakulta
Katedra obrábania a výrobnej techniky

Školiteľ: prof. Ing. Andrej Czán, PhD.
Žilinská univerzita v Žiline
Strojnícka fakulta
Katedra obrábania a výrobnej techniky

Oponenti:

1. Dr.h.c. prof. Ing. Michal Hatala, CSc. TU Košice
2. doc. Ing. Peter Križan, PhD. - STU Baratislava
3. doc. Ing. Štefan Václav, PhD. STUBA MTF so sídlom v Trnave

Autoreferát bol rozoslaný dňa:

Obhajoba dizertačnej práce sa koná dňa 31.08.2026 o 12:00 hod. v miestnosti PP122 na SjF, Univerzitná 8215/1, 010 26, Žilina, pred komisiou pre obhajobu dizertačnej práce schválenou odborovou komisiou v študijnom odbore Strojárstvo, v študijnom programe Automatizované výrobné systémy, vymenovanou dekanom Strojníckej fakulty, Žilinskej univerzity v Žiline.

S dizertačnou prácou je možné sa oboznámiť na referáte pre vedu a výskum dekanátu SjF, UNIZA, Univerzitná 8215/1, 010 26 Žilina.

prof. Dr. Ing. Ivan Kuric v. r.
predseda komisie pre obhajobu dizertačnej práce

INTRODUCTION

Additive manufacturing has, in the last two decades, evolved from a tool of rapid prototyping into a recognised industrial production technology. The principle of building components layer by layer offers a high degree of design freedom and allows the realisation of geometries that are either difficult or entirely impossible to produce by conventional subtractive routes. The interaction between part design, internal architecture, material behaviour and the manufacturing process has therefore become a central research subject of contemporary production engineering.

Among the design features that additive manufacturing has made readily accessible, lattice structures occupy a particularly prominent position. By replacing fully dense material with a periodic cellular architecture, lattices simultaneously reduce part mass, increase the available surface area, and tailor the mechanical response of the component to the specific loading scenario. They have become a key enabler for lightweight engineering in aerospace, automotive, biomedical and protective applications, where the simultaneous optimisation of mass, stiffness, strength and energy-absorption capacity is required.

Despite their growing industrial relevance, the mechanical response of additively manufactured lattices cannot be predicted from topology alone. The choice of manufacturing process, the consolidation mechanism of the feedstock, the dimensional evolution of the part during post-processing and the manufacturing-induced defects all enter the macroscopic response and may dominate over the inherent efficiency of the cellular geometry. A rigorous understanding of lattice behaviour therefore requires the topology, the material and the manufacturing process to be examined jointly, rather than as independent design variables.

The present dissertation addresses this requirement through an integrated experimental and statistical investigation of polymer and metal lattice structures produced by representative additive manufacturing technologies. The polymer campaign compares Selective Laser Sintering (SLS) on the EOS Formiga P 110 Velocis platform with Multi Jet Fusion (MJF) on the HP Jet Fusion 5200 platform, using PA 12 powders that are nominally identical in chemistry but differ markedly in consolidation route. The metal campaign explores Atomic Diffusion Additive Manufacturing (ADAM) on the Markforged Metal X platform with 17-4 PH precipitation-hardenable stainless steel and delimits the manufacturing envelope of this filament-based metal process for cellular geometries.

The theoretical part of the work establishes the necessary framework for the experimental investigation: the historical development and current state of additive manufacturing, the consolidation principles of the selected powder-bed and bound-metal processes, the classification of lattice topologies into strut-based and surface-based (TPMS) categories, and the characteristic compressive response of cellular solids according to ISO 13314. The experimental part presents the design of the test specimens, the fabrication on three different platforms, the compression-testing programme, and the statistical evaluation of the recorded responses by analysis of variance and least-squares modelling in JMP, complemented by desirability optimisation through the Prediction Profiler. The findings obtained provide both engineering recommendations for the selection of lattice–process combinations and a methodological basis for the continued development of metal lattice research.

1 ADDITIVE MANUFACTURING OF POLYMERS AND METALS

Additive manufacturing (AM) is one of the most significant innovations within modern production engineering. Its development has introduced a fundamentally new approach to the design and fabrication of components, in which complex geometries with internal cavities, undercuts and graded architectures can be produced directly from the digital model without the need for dedicated tooling. Compared with conventional subtractive routes, AM offers more efficient material utilisation, shorter product-development cycles and economic small-batch and individualised production [1, 2].

The significance of additive manufacturing has been steadily growing as the range of processable materials expands and as the underlying machines and software environments mature. Active research nevertheless continues to address productivity, process-parameter optimisation and the simultaneous achievement of high dimensional accuracy and favourable production economics [3].

Among the historically earliest commercial AM technologies, stereolithography (SLA) made a decisive contribution to the development of rapid prototyping and opened the way for subsequent process families [4]. Material extrusion (commonly referred to as Fused Deposition Modelling, FDM, or Fused Filament Fabrication, FFF) followed shortly and has since become one of the most widely adopted polymer AM processes thanks to its simplicity, the variety of available feedstocks and the favourable operating cost [5].

With the maturation of the field, the attention of both manufacturers and research institutions gradually shifted from the processing of polymeric feedstocks to the production of metallic components. This trend has been driven by the demand for functional parts with high mechanical performance, tight dimensional accuracy and long-term operational reliability. Powder-bed fusion technologies, in particular Selective Laser Melting (SLM), have consequently undergone intensive development and now permit the fabrication of geometrically complex metal components for aerospace, automotive, energy and biomedical applications [2, 6].

A complementary route to metal AM is provided by indirect, multi-stage processes that combine extrusion-type deposition of a metal-loaded composite feedstock with subsequent debinding and sintering. Atomic Diffusion Additive Manufacturing (ADAM), developed by Markforged, is the principal representative of this family and constitutes the central metallic technology of the present dissertation. ADAM offers substantially lower acquisition and operating costs than laser-based powder-bed fusion and is, in principle, attractive for laboratories and small enterprises that wish to introduce metal AM without the capital outlay associated with SLM-class equipment.

The dynamic development of additive manufacturing, supported by improvements in feedstocks and in slicing and toolpath-generation software, continues to enlarge the range of components for which AM represents an economically and technically competitive production route. The lattice structures investigated in the present dissertation belong precisely to the class of design features whose practical use depends on the simultaneous availability of an appropriate topology, an appropriate material and an appropriate manufacturing process.

2 CURRENT STATE OF POLYMER AND METAL ADDITIVE MANUFACTURING TECHNOLOGIES

This chapter summarises the additive manufacturing technologies that are directly relevant to the experimental investigation. Two polymer powder-bed fusion processes — SLS and MJF — are described together with the bound-metal ADAM process used in the metallic part of the campaign. The selection reflects the practical scope of the dissertation, namely a systematic comparison of two industrially significant PBF routes for polymer lattices and a feasibility-level investigation of ADAM for metallic lattices.

2.1 Selective Laser Sintering (SLS)

Selective Laser Sintering belongs to the family of powder-bed fusion processes and is one of the most established additive manufacturing technologies for polymer components. A thin layer of polymer powder, typically PA 12, is deposited on a pre-heated build platform and selectively consolidated by a focused CO_2 laser beam operating at 10.6 µm, a wavelength at which polyamide 12 exhibits a high natural absorption efficiency. After the consolidation of one layer, the build platform is lowered by the chosen layer thickness, a fresh layer of powder is spread by a recoater blade or roller, and the cycle repeats until the build is complete.

A defining feature of SLS is that the loose, unsintered powder surrounding each printed cross-section acts as a self-supporting bed. Overhangs, undercuts and internal cavities can therefore be produced without the dedicated support structures required by extrusion-type processes. This property is particularly important for lattice structures, in which the cellular interior cannot be accessed for mechanical support removal.

The principal SLS platform used in the present dissertation is the EOS Formiga P 110 Velocis with EOS PA 2200 (a white PA 12). The system delivers a high degree of particle consolidation, fully dense walls and a predominantly ductile macroscopic response of the printed component.

2.2 Multi Jet Fusion (MJF)

Multi Jet Fusion, developed by Hewlett-Packard, is a more recent powder-bed fusion technology that consolidates a polymer powder by an indirect, agent-mediated route. Instead of a focused laser beam, MJF uses a moving carriage that selectively deposits a carbon-based fusing agent on the regions to be solidified, together with a detailing agent that limits the lateral spreading of the consolidation front. Planar infrared radiation then heats the entire powder bed; the fusing agent absorbs the radiation and converts it into thermal energy that is transferred to the surrounding polymer grains by conduction.

The resulting consolidation is faster than in SLS and produces parts with characteristically dark grey to black colour, owing to the residual carbon black of the fusing agent. The degree of particle melting, and consequently the local density and the macroscopic stiffness and strength of the consolidated material, is systematically different from that of laser-sintered PA 12, and these differences are one of the central subjects of the polymer experimental campaign.

The MJF system used in the present dissertation is the HP Jet Fusion 5200 with HP 3D High Reusability PA 12 (a dark grey PA 12).

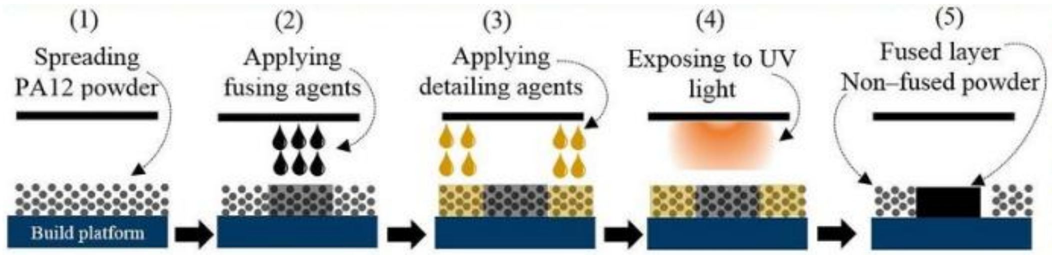

Figure 2.1 Schematics of HP MJF Process

2.3 Atomic Diffusion Additive Manufacturing (ADAM)

ADAM is a bound-metal extrusion technology developed by Markforged and is the metallic AM process used in the present dissertation. Unlike laser-based powder-bed fusion of metals, ADAM does not melt the metal powder directly during deposition. Instead, a composite filament consisting of metal powder embedded in a sacrificial polymer matrix is extruded layer by layer in a process that closely resembles polymer fused-filament fabrication. The resulting so-called green part is geometrically over-sized by approximately 20 % to compensate for the subsequent shrinkage during sintering.

The green part is then transferred to a solvent debinding station (Markforged Wash-1), in which the soluble fraction of the polymer binder is removed, leaving the so-called brown part. The brown part retains its full geometric form but is held together only by the residual polymer binder and is therefore extremely brittle. The final operation is sintering in a controlled-atmosphere furnace (Markforged Sinter-2), in which the part is heated to the order of 1300 °C, the residual binder is volatilised, and the metal particles diffuse across their mutual contacts to form a fully consolidated metallic component. During this stage the part contracts approximately isotropically to its design dimensions.

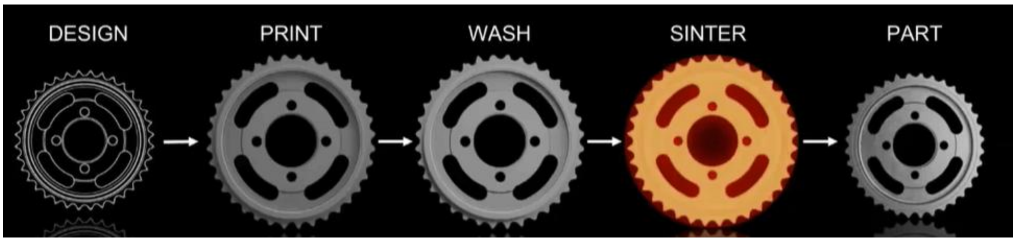

Figure 2.2 Markforged ADAM process example

ADAM imposes several specific design constraints that differ markedly from those of powder-bed fusion. Overhangs beyond approximately 45° require support material that is deposited as a second filament, with a thin ceramic-release interlayer between the load bearing and the support material to prevent metallurgical bonding during sintering. Unsupported horizontal bridges are limited by the rheology of the molten metal-loaded composite filament. These constraints become particularly restrictive for three-dimensional cellular geometries, where the cumulative requirement of internal support quickly exceeds the post-process removability of the deposited support assembly.

3 AIMS OF THE WORK

The main aim of the dissertation thesis is the experimental and statistical investigation of lattice structures manufactured by additive technologies, with a focus on the influence of unit-cell topology, cell size and the selected manufacturing process on the macroscopic mechanical response of the printed specimens. The work covers both polymer and metal feedstocks and explicitly addresses the boundary between the two material classes by treating the manufacturing process as a primary experimental factor on a par with topology and cell size.

On the polymer side, the work compares three lattice topologies — the body-centred-cubic (BCC) strut topology and the Gyroid and Schwarz Diamond triply periodic minimal surfaces (TPMS) — at three cell sizes (6, 7.5 and 9 mm) produced by two powder-bed fusion processes, SLS on the EOS Formiga P 110 Velocis with EOS PA 2200 and MJF on the HP Jet Fusion 5200 with HP 3D High Reusability PA 12. The resulting design space spans 54 specimens, distributed according to a Taguchi L27 orthogonal array generated in Minitab 17, and is evaluated by quasi-static compression testing according to ISO 13314.

On the metal side, the work investigates the feasibility of producing geometrically equivalent lattice structures by Atomic Diffusion Additive Manufacturing on the Markforged Metal X system with 17-4 PH precipitation-hardenable stainless steel. The principal objective of this part of the campaign is to map the manufacturing envelope of ADAM for cellular geometries, to identify the topologies and orientations that can be realised within this envelope, and to derive on that empirical basis a structured proposal for a follow-up study comparing ADAM with Selective Laser Melting (SLM) on a common metal feedstock.

The methodological aim of the work is the development of an integrated evaluation framework that combines the design of experiments, classical analysis of variance and least-squares modelling with diagnostic residual analysis, Box–Cox transformation and Prediction-Profiler-based desirability optimisation. The same framework is applied to all responses examined in the dissertation, so that the polymer and metal campaigns become directly comparable at every level of the statistical analysis. A dedicated volume-specific response, the volumetric force $f = F / V$, is introduced to enable a topology-independent and size-independent comparison of lattices that differ in their internal architecture and in their consolidated mass.

The expected outcomes of the dissertation are: a quantitative characterisation of the relative contributions of topology, cell size and manufacturing process to the compressive response of polymer lattices; a transparent and reproducible methodology for the design and statistical evaluation of comparable AM experiments; and a justified delimitation of the manufacturing envelope of ADAM for lattice structures, accompanied by a structured outline of the recommended follow-up investigation. Beyond their immediate scientific value, the results are intended to support the selection of lattice–process combinations in the aerospace, automotive, biomedical and protective-equipment sectors, where additively manufactured cellular components are increasingly being deployed.

4 TECHNOLOGY SELECTION FOR THE EXPERIMENT

4.1 Manufacturing technologies used in the experiment

For the experimental part of the dissertation, three additive manufacturing technologies were selected. Two powder-bed fusion processes — Selective Laser Sintering (SLS) and Multi Jet Fusion (MJF) — were used for the polymer lattice campaign, while Atomic Diffusion Additive Manufacturing (ADAM) was used for the metallic feasibility campaign. The selection reflects both the industrial significance of these technologies and the structure of the research questions formulated in the previous chapter.

SLS and MJF were chosen because they jointly represent the two dominant consolidation routes of polymer powder-bed fusion: direct laser-driven melting (SLS) and indirect, infrared-driven, agent-mediated fusion (MJF). They process a nominally identical PA 12 chemistry but differ markedly in the degree of particle consolidation, in the resulting macroscopic ductility and in the characteristic colour of the consolidated part. They therefore allow the contribution of the manufacturing process to be isolated from the contribution of the topology and the cell size on a chemically controlled material basis.

ADAM was chosen as the representative metal AM process because it is currently the most accessible bound-metal AM technology for laboratory environments, because it offers substantially lower acquisition and operating costs than laser-based powder-bed fusion of metals, and because its application envelope for cellular geometries has not been systematically characterised in the published literature.

4.2 Polymer feedstocks: PA 12 from SLS and MJF

The polymer specimens were produced from polyamide 12 (PA 12) in two distinct realisations: a white PA 12 (EOS PA 2200) processed by laser-driven SLS on the EOS Formiga P 110 Velocis, and a dark grey PA 12 (HP 3D High Reusability PA 12) processed by infrared-driven MJF on the HP Jet Fusion 5200. PA 12 was selected because of its industrial relevance, its favourable balance between strength, ductility and processability, and its established use as the reference material of both SLS and MJF platforms.

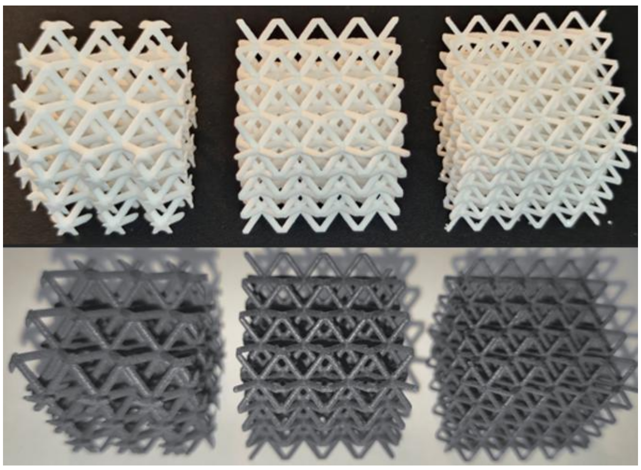

Figure 4.1 Comparison of white PA12 powder (EOS PA 2200, top) and dark PA12 powder with carbon black (HP PA12, bottom)

In the present statistical evaluation, the two polymer materials are coded as W for the white EOS PA 2200 and B for the dark HP PA 12, the latter designation reflecting the presence of carbon black associated with the MJF fusing agent. The two materials are nominally identical in chemistry but differ in their as-printed consolidation density and in the characteristic ductility of the consolidated solid, with material W exhibiting the more ductile, fully consolidated response and material B the more brittle response associated with the lower degree of particle melting.

4.3 Metal feedstock: 17-4 PH precipitation-hardenable stainless steel

The metallic specimens were produced from 17-4 PH precipitation-hardenable stainless steel deposited as a metal-loaded composite filament on the Markforged Metal X system. 17-4 PH was selected because it is the most established metal feedstock of the ADAM platform, because it combines a high mechanical strength with a favourable corrosion resistance, and because qualified material data exist for it across a broad range of metal AM processes, which makes it a natural candidate for the cross-technology follow-up study outlined in Chapter 8 of the dissertation. The chemical composition of the alloy is summarised in Table 4.1.

Table 4.1 — Chemical composition of 17-4 PH precipitation-hardenable stainless steel

Composition	Element	Content (%)
Steel 17-4 PH	Chromium (Cr)	15 – 17.5
	Nickel (Ni)	3 – 5.1
	Copper (Cu)	3 – 5.1
	Manganese (Mn)	max. 1
	Silicon (Si)	max. 1
	Niobium (Nb)	0.15 – 0.45
	Phosphorus (P)	max. 0.04
	Carbon (C)	max. 0.07

Owing to the combination of favourable mechanical properties and high corrosion resistance, 17-4 PH belongs among the principal structural materials used in modern manufacturing technologies and industrial applications with demanding reliability and lifetime requirements. The alloy exhibits high strength, good wear resistance, and stability under elevated service temperatures, and is suitable for a broad range of manufacturing processes including welding, machining and additive manufacturing. Within the Markforged Metal X system, 17-4 PH represents the most widely used feedstock and is supported by stable, long-term qualified process parameters provided by the equipment manufacturer.

5 DESIGN AND FABRICATION OF EXPERIMENTAL SPECIMENS

5.1 Concept of the test specimens

The experimental specimens were designed in accordance with ISO 13314, the international standard for the compressive characterisation of porous and cellular materials. All specimens adopted uniform external dimensions of 30 × 30 × 30 mm, into which the internal lattice geometry was generated according to the chosen topology and cell size. ISO 13314 recommends a specimen-size-to-cell-size ratio of at least 1:10; this requirement is fully satisfied for the 6 mm cell only, while it is satisfied partially for the 7.5 mm and 9 mm cells. The cell sizes were nevertheless retained as a deliberate experimental factor for assessing the sensitivity of the responses to the cell-size dimension.

Three lattice topologies were selected for the experiment, covering the two principal categories of unit-cell geometry. The body-centred-cubic (BCC) lattice represents the strut-based, bending-dominated family. The Gyroid and the Schwarz Diamond represent the surface-based, triply periodic minimal-surface (TPMS) family with smoothly curved, mathematically defined walls. The three topologies allow a direct comparison between strut-based and surface-based geometries, and a comparison of two different TPMS families against each other.

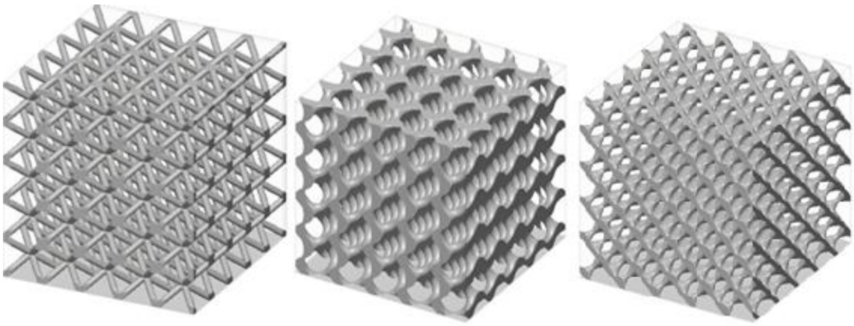

Figure 5.1 CAD models of the three lattice topologies: BCC (strut-based), Gyroid (TPMS) and Schwarz Diamond (TPMS)

5.2 Cell-size selection and adjustments arising from the print trials

The initial design intent envisaged cell sizes of 3, 4.5 and 6 mm, to span a wide range of relative density. The print trials on the EOS Formiga P 110 Velocis with white PA 12 (PA 2200), however, exposed a recurrent failure mode of the smallest cells: partially built struts and walls were swept away by the recoater blade, the build was interrupted and the partially printed specimens were destroyed. The cause was identified as the insufficient mechanical stability of thin struts during deposition, in combination with the adhesion of the partially built features to the moving recoater. On the HP Jet Fusion 5200 with dark PA 12 the print itself succeeded, but the specimens could not be cleaned of trapped powder during depowdering, and the post-processing yield was correspondingly poor.

Based on these trials, the cell sizes were revised to 6, 7.5 and 9 mm, which are reliably manufacturable on both platforms, and which still provide a meaningful resolution of the cell-size effect on the macroscopic response. The relative density of all specimens was held constant at a solidity of 0.2, so that the cell-size factor describes the geometric scaling of the unit cell at constant material fraction rather than a confounded combination of size and density.

5.3 Manufacturing on the EOS Formiga P 110 Velocis and HP Jet Fusion 5200

The polymer specimens were prepared in Materialise Magics 27 and processed in the dedicated build-preparation environments of the two platforms. On the EOS Formiga P 110 Velocis the layer thickness was set to 0.1 mm, and the standard EOS PA 2200 process parameter set was applied. On the HP Jet Fusion 5200 the layer thickness was set to 0.08 mm, and the standard HP 3D High Reusability PA 12 parameter set was used. In both cases the specimens were arranged within the build chamber to avoid orientation-related artefacts in the comparison between the two systems.

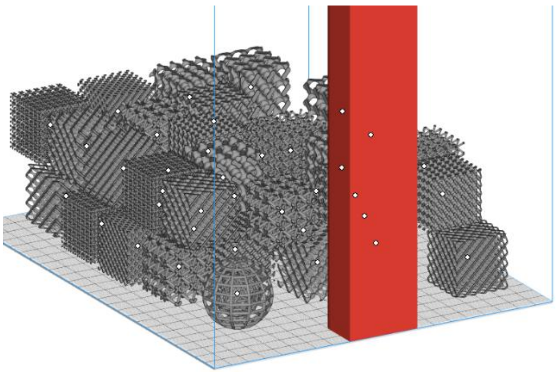

Figure 5.2 Build preparation in Materialise Magics: arrangement of compression specimens within the build chamber

After printing, the specimens were cooled within the build chamber, removed from the cake of unsintered powder, brushed and lightly bead-blasted in the unpacking stations of the respective platforms. No further post-processing was applied so as not to introduce a confounding variable into the comparison between the two platforms.

5.4 Metal specimens for the ADAM feasibility campaign

The metal specimens were redesigned for the ADAM process. Because ADAM inherits from fused deposition modelling the basic geometric constraints of viscous-filament deposition under gravity, the bare lattice geometry adopted for the polymer specimens cannot be transferred directly to the Metal X system. A sandwich-plate architecture was therefore adopted, in which the lattice volume is enclosed between two fully dense flat plates, integrally printed as part of the same build. The plates provide the planar bearing surfaces required by ISO 13314 and simultaneously reinforce the upper and lower terminations of the cellular volume.

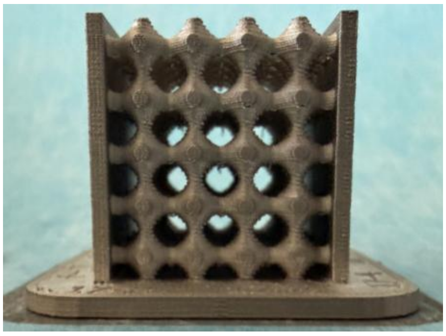

Figure 5.3 Side view of a successfully sintered ADAM specimen illustrating the sandwich-plate architecture

Each specimen carries a dedicated raft with the alphanumeric designation "17-4" — referring to the 17-4 PH chemistry of the deposited feedstock — together with individual identifiers permitting the unambiguous traceability of each specimen through the print, wash and sinter stages. The lateral faces of the specimens were left open so that the support material in the lattice interior could in principle be removed after sintering, and so that the deformation of the cellular volume could be observed optically during the subsequent compression tests.

6 MECHANICAL COMPRESSION TESTING AND RESULTS

6.1 Test equipment and procedure

Quasi-static compression testing was carried out on a Zwick/Roell Z150 universal testing machine with a 150 kN load cell, in accordance with ISO 13314. The specimens were placed centrally between two flat parallel compression platens; the upper platen being mounted in a self-aligning fixture to compensate for residual non-parallelism between the bearing surfaces. The crosshead speed was set to 5 mm/min, corresponding to a nominal strain rate of approximately 2.8×10^{-3} s^{-1} for the 30 mm specimens, which lies well within the quasi-static regime defined by ISO 13314.

Figure 6.1 Zwick/Roell Z150 universal testing machine

The recorded force–displacement traces were converted to engineering stress and engineering strain through the standard relations $\sigma = F / S_0$ and $\varepsilon = \Delta l / h_0$, in which S_0 is the initial nominal cross-section of the bounding envelope and h_0 is the initial specimen height. The principal response variables extracted from each curve are the quasi-elastic gradient EC, the first peak compressive stress σ_{peak}, the plateau stress σ_{pl} evaluated as the average stress between 20 % and 30 % strain, and the volumetric energy absorption W evaluated as the integral of stress over strain up to the densification onset.

6.2 Stress–strain response of the polymer lattices

The polymer compression tests were carried out on the full set of 54 specimens, organised into eighteen groups according to topology, cell size and printer. The principal qualitative observations can be summarised as follows.

The BCC lattice exhibits a smooth, bending-dominated response without a pronounced first maximum, characteristic of strut-based topologies that deform through bending of the inclined struts. The Gyroid lattice exhibits the typical membrane-stress-dominated response of TPMS structures, with a steep linear-elastic region, a pronounced first maximum and an extended plateau region. The Schwarz Diamond lattice exhibits the largest scatter between repetitions of all three topologies, with oscillatory plateau regions and, for the HP material, with brittle fracture before the densification region is reached.

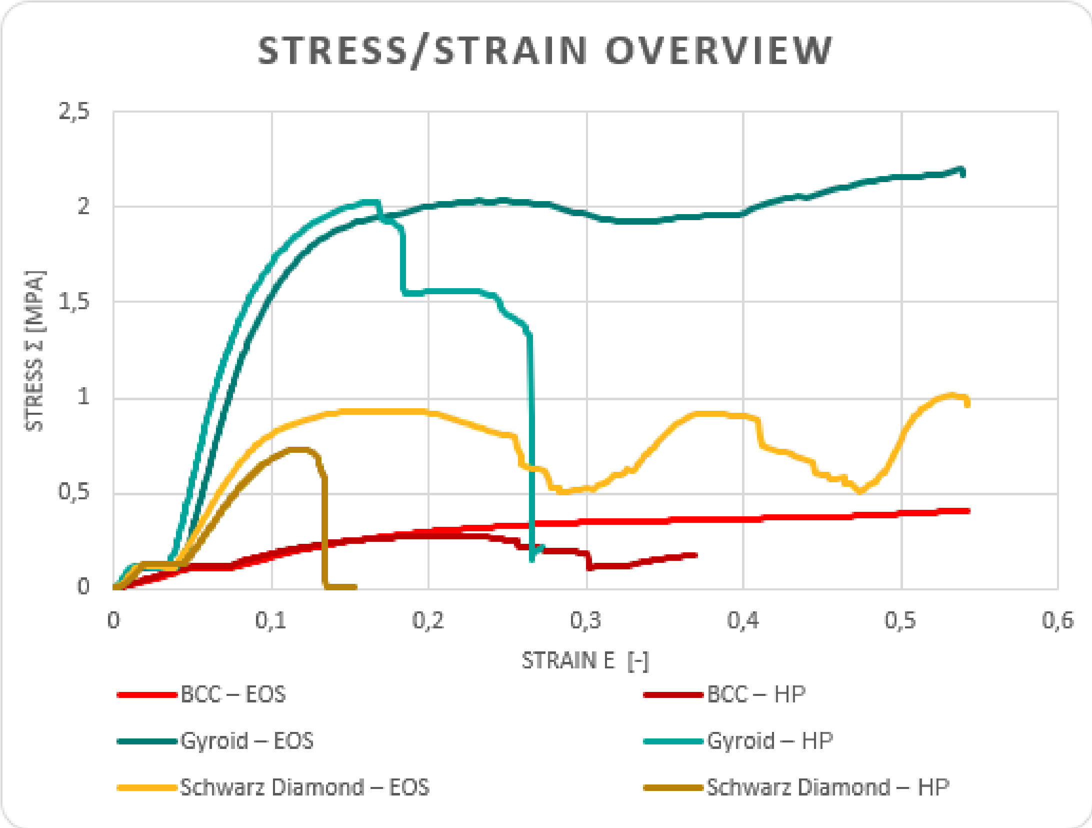

Figure 6.2 Representative stress–strain curves for all six material-topology combinations (9 mm cell)

Across all topologies, the EOS specimens (white PA 12) systematically reach higher plateau stress and higher specific energy absorption than the HP specimens (dark PA 12), reflecting the more ductile, fully consolidated response of laser-sintered PA 12 in comparison with the agent-fused PA 12 of MJF. The HP specimens, by contrast, exhibit a slightly higher initial stiffness for the Schwarz Diamond and Gyroid topologies, which reflects the higher modulus of the matrix material associated with the residual carbon black of the MJF fusing agent.

6.3 Manufacturing outcomes of the ADAM campaign

The metallic feasibility campaign produced a strongly topology-dependent yield. Simple strut-based lattices oriented for minimum overhang yielded close to 100 % of the attempted specimens, with cleanly defined cellular geometries and fully dense sandwich plates. Strut-based lattices in unfavourable orientations and Schwarz-P-like derivatives yielded approximately half of the attempted specimens. Triply periodic minimal-surface topologies, by contrast, yielded essentially no specimens of testable quality in any of the orientations explored.

Figure 6.4 Defective lattice specimen illustrating the principal ADAM failure modes: partial blockage of the cellular volume by residual support material, localised strut collapse and fusion, and sagging of the upper sandwich plate

Inspection of the build preparation in the Markforged Eiger slicer revealed that the algorithm, when applied to a cellular interior, generates support and ceramic-release material throughout the volume that the lattice is by design intended to leave empty. The resulting build is, in effect, a fully dense block in which the porosity of the design intent has been replaced by sintered support and ceramic residue, and the cellular topology contributes nothing to the mechanical response of the part. A manual override sketch can be applied to suppress support generation within a selected band of layers, but the slicer treats the override as an unconditional instruction and does not verify whether the load-bearing geometry can be deposited without support. The geometric viability of the cellular interior is therefore gambled on each build cycle and confirmed only retrospectively, after the full debinding-and-sintering sequence has been completed.

Based on these observations, the ADAM process is characterised as a viable manufacturing route for simple, support-tolerant cellular geometries in 17-4 PH stainless steel, but an unsuitable route for the geometrically demanding lattice topologies that offer the highest specific mechanical performance. A structured comparison with Selective Laser Melting on a common metal feedstock is proposed as the natural continuation of the metallic part of the work.

7 STATISTICAL EVALUATION OF EXPERIMENTAL DATA BY DOE METHODS

7.1 ANOVA evaluation of the polymer responses

The statistical evaluation of the polymer compression data was carried out in two complementary tiers. The first tier applies a classical analysis of variance (ANOVA) within a general linear model (GLM) in Minitab 17. For each of the four principal responses — the quasi-elastic gradient EC, the first peak stress σ_{peak}, the plateau stress σ_{pl} and the volumetric energy absorption W — the sum of squares attributable to each main factor and to the admissible two-factor interactions was decomposed and tested for statistical significance against a residual term. The summary of the ANOVA results is given in Table 7.1.

Table 7.1 ANOVA (GLM) results for all four monitored responses

Factor	E_c [MPa]	σ_{peak} [MPa]	σ_{pl} [MPa]	W [MJ/m³]
	F p	*F p*	*F p*	*F p*
Structure type	255.1 0.000	355.6 0.000	113.4 0.000	74.95 0.000
Cell size	3.51 0.038	7.39 0.002	2.57 0.089	3.70 0.032
Printer	21.6 0.000	3.39 0.072	24.9 0.000	45.62 0.000
R^2	**91.82 %**	**93.83 %**	**86.04 %**	**80.87 %**

The structure type emerges as the statistically most significant factor for all four responses, with F-values orders of magnitude higher than those of the cell size and printer. The coefficient of determination R^2 ranges between 80 % and 94 %, indicating that the linear model explains the predominant part of the variability of the data. The cell size emerges as statistically significant for EC and σ_{peak} but not for σ_{pl}, whereas the printer effect is significant for EC, σ_{pl} and W. The σ_{peak} response stands out as the only response on which the printer effect is not significant, which is consistent with the geometric interpretation that the first peak load is determined primarily by the geometry of the structure rather than by the consolidation route of the matrix.

7.2 Least-squares analysis and the volumetric force f

The second tier of the statistical evaluation applies the Least Squares Fit platform of JMP to the same data set. The model includes three categorical factors — Structure (G, S, X), Size (6, 7.5, 9 mm) and Materials (B, W) — together with all their two-factor and three-factor interactions. Three response variables are examined in parallel: the recorded peak compressive force F (Data points, kN), the nominal lattice volume V (dm^3), and the volume-specific force $f = F / V$ (kN/dm^3).

The volumetric force f is introduced because the conventional engineering stress $\sigma = F / A$, which refers the recorded force to the cross-sectional area of the bounding envelope, is a structure-dependent rather than a material-dependent quantity for porous specimens: two lattices of identical polymer chemistry can yield very different nominal stresses simply because they differ in unit-cell topology or in relative density. Referring the recorded force to the nominal CAD volume instead removes the dependence on the bounding cross-section and provides a topology-independent and size-independent basis for comparing lattices of different internal architecture. Dimensionally, f is a force density and is reported throughout the present analysis in kN/dm^3.

Source	Logworth	PValue
Materials	10,550	0,00000
Structure	7,434	0,00000
Structure*Materials	6,340	0,00000
Size*Materials	0,858	0,13857
Size	0,845	0,14302
Structure*Size	0,622	0,23905
Structure*Size*Materials	0,516	0,30473

Figure 7.1 Effect Summary plot ranking the sources of variability of the peak compressive force by their LogWorth values (JMP output)

The Effect Summary for the peak compressive force confirms the picture established by the ANOVA: the factor Materials reaches the highest statistical significance ($F = 89.14$, $p < 0.0001$), followed by Structure ($F < 0.0001$) and by the Structure × Materials interaction ($F = 22.51$). The factors Size and all its interactions with the remaining factors are statistically not significant within the explored 6 – 9 mm range. The same hierarchy of effects is recovered for the volumetric force f, with Materials ($F = 82.53$), Structure and the Structure × Materials interaction ($F = 22.26$) dominating the model, and Size remaining non-significant. The consistency of the two analyses substantially strengthens the credibility of the identified relationships and demonstrates that the dominant effects are not artefacts of the cross-section normalisation.

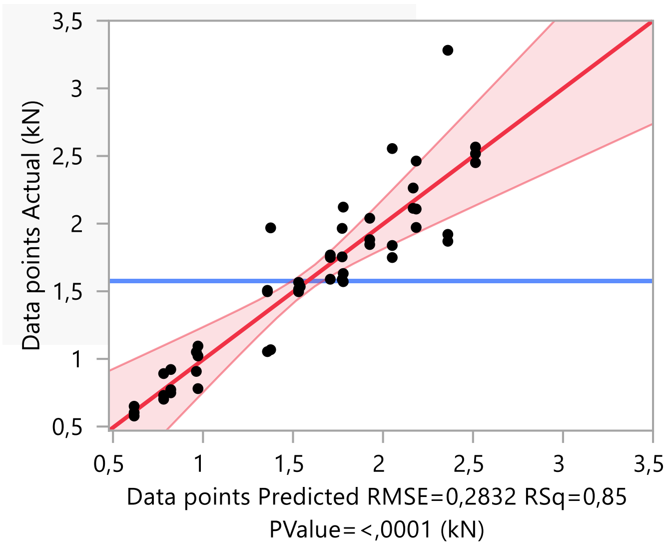

Figure 7.2 Actual-by-Predicted plot for the peak compressive force showing the model fit, the 1:1 reference line and the 95 % mean confidence band

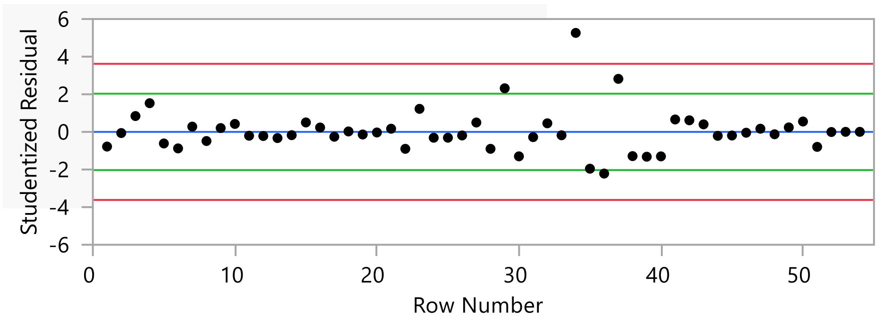

Figure 7.3 Residual-by-Predicted and externally studentized residuals plots for the peak compressive force, used to verify the assumptions of the linear model

The diagnostic plots confirm a good agreement of the model with the measured data, a uniform distribution of the residuals around the zero line, and the absence of outliers exceeding the 95 % simultaneous Bonferroni limits. The Box–Cox transformation diagnostic returns $\lambda \approx -0.359$ for the peak force and $\lambda \approx -0.755$ for the volumetric force, indicating that the original-scale model already satisfies its assumptions and that the suggested transformations would represent refinements only.

7.3 Prediction Profiler and desirability optimisation

The least-squares model was used to drive the Prediction Profiler of JMP, in which the desirability function permits the simultaneous optimisation of the response variables across the entire factor space. Two limiting configurations were explored: the minimum-response configuration, which identifies the combination of factors that yields the lowest predicted response, and the maximum-response configuration, which identifies the combination that yields the highest predicted response.

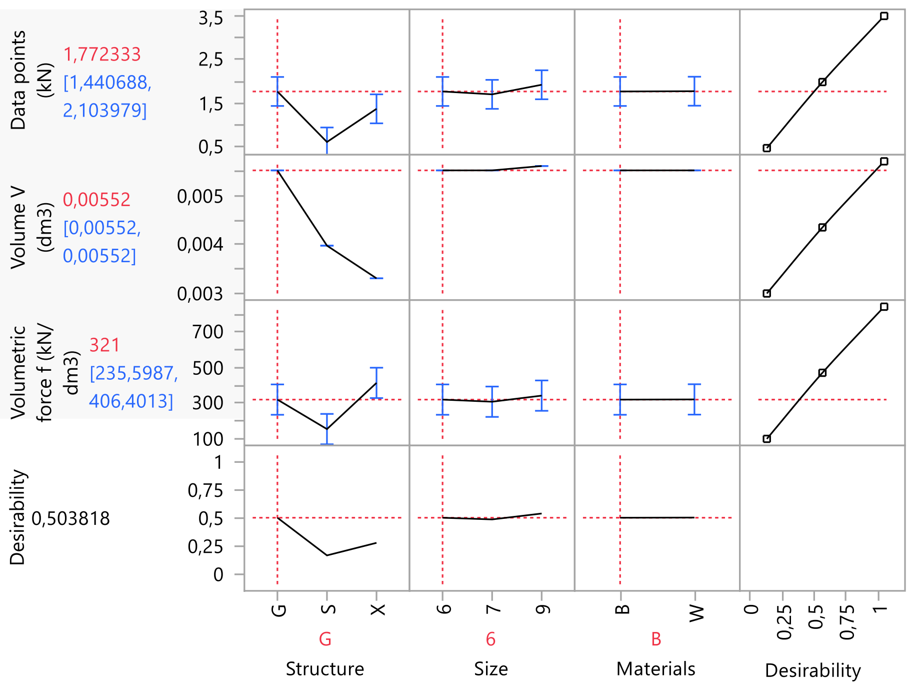

Figure 7.4 — Prediction Profiler for the minimum-response configuration (structure S, size 9, material B)

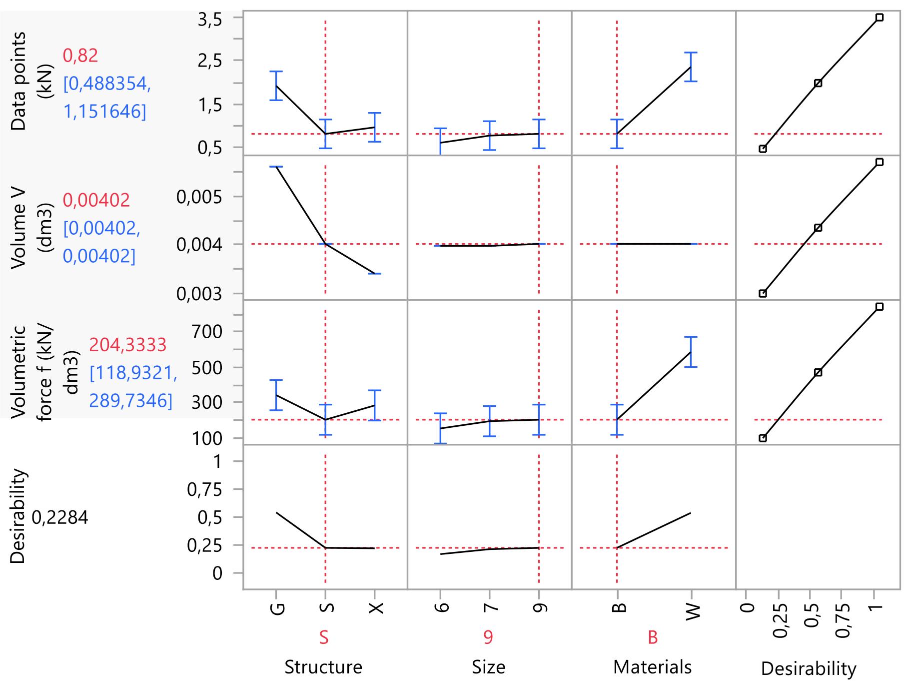

Figure 7.5 — Prediction Profiler for the maximum-response configuration (structure G, size 9, material W)

The minimum-response configuration is identified as Schwarz Diamond (S) at the 9 mm cell with material B (HP MJF), with a predicted peak force of approximately 0.74 kN. The maximum-response configuration is identified as Gyroid (G) at the 9 mm cell with material W (EOS SLS), with a predicted peak force of approximately 2.36 kN. The three-fold contrast between the two configurations is consistent with the dominant role of the Materials main effect and of the Structure × Materials interaction in the underlying statistical model. The recommended lattice–process combination for maximum specific load-carrying capacity is therefore the Gyroid topology produced by laser-driven SLS on the EOS platform, while the BCC topology produced on the same platform is identified as the appropriate choice when a low initial stiffness and a progressive, ductile collapse without sudden failure are desired.

7.4 Summary of the statistical evaluation

The combined two-tier statistical evaluation, carried out by ANOVA in Minitab 17 and by least-squares modelling in JMP, identifies three substantive effects on the mechanical response of the printed polymer lattices: a dominant effect of the material (consolidation route), a comparable effect of the unit-cell topology and a strong Structure × Materials interaction. The cell size, by contrast, emerges as statistically not significant within the explored 6 – 9 mm range at constant solidity, so that the structure–material combination can be selected on mechanical grounds without further constraint from the cell-size dimension, provided that the minimum-cell-count requirement of ISO 13314 is respected.

8 DISCUSSION

The results of the statistical evaluation admit a coherent physical interpretation in terms of the consolidation mechanisms of the two-polymer powder-bed fusion processes and the load-bearing behaviour of the three lattice topologies. The dominant effect of the Materials factor reflects the fundamental difference between the two consolidation routes. The EOS architecture (material W) employs a CO_2 laser at 10.6 µm, a wavelength at which PA 12 absorbs the radiation with high natural efficiency, and the polymer powder is consequently melted directly to a high degree of particle coalescence. The HP architecture (material B) relies on indirect, agent-mediated heating, in which planar infrared radiation is converted into thermal energy by the carbon-based fusing agent and transferred to the polymer grains by conduction. The resulting degree of particle melting, and therefore the local density of the consolidated material, is systematically lower for MJF than for laser SLS on the same nominal PA 12 chemistry. The 60 % higher mean peak force observed for material W is fully consistent with this picture, and the preservation of the W-versus-B gap across all topologies and cell sizes strengthens the causal interpretation.

The ranking of the three structure types — Gyroid > Schwarz Diamond > BCC — is in good agreement with the established mechanics of cellular solids. The Gyroid is a triply periodic minimal surface with smooth, continuously curved walls and no point-like stress concentrators; under uniaxial compression a substantial fraction of its surface deforms in a stretch-dominated regime that yields higher specific stiffness and strength than the bending-dominated regime of strut-based lattices of comparable relative density. The Schwarz Diamond is likewise a TPMS, but its connecting necks are thinner, and its load paths are more bending dominated than those of the Gyroid, which moves it to an intermediate position. The body-centred-cubic strut topology places its load-bearing elements between point-like junctions at the cell corners; these junctions concentrate stress and the struts deform predominantly in bending, which is why this topology systematically delivers the lowest specific response.

The Structure × Materials interaction is the most informative finding of the analysis. The combination Schwarz Diamond–W produced the highest mean response of the entire data set (2.198 kN), while the combination Schwarz Diamond–B produced the lowest (0.739 kN) — a three-fold contrast that cannot be explained by the individual main effects alone. The physical interpretation is that the Schwarz Diamond, with its thin connecting necks, is the most demanding of the three structures from a manufacturing point of view: small defects, partially fused particles or local under-consolidation in these critical cross-sections translate into a disproportionately large reduction of the macroscopic load-carrying capacity. Laser SLS, which delivers fully consolidated walls, expresses the inherent mechanical efficiency of the topology; MJF, which exhibits a lower degree of particle melting in the same thin cross-sections, collapses at a much lower load. The interaction is, in other words, a manifestation of process–structure coupling: the relative advantage of laser SLS over MJF grows with the geometric demand placed on the process by the lattice topology.

The non-significance of the cell size within the explored 6 – 9 mm range is consistent with the geometric scaling argument for cellular solids. If the relative density is held constant, a proportional increase of the unit-cell size leaves the topology, the load paths and the local stress distribution unchanged, and the macroscopic response per unit volume is therefore preserved. The non-significance of Size represents a useful experimental result, since it implies that the cell size can be selected based on design criteria such as part mass, surface-to-volume ratio or manufacturability without an appreciable penalty on the macroscopic mechanical response.

The metallic part of the dissertation, by contrast, demonstrates that the geometric and statistical conclusions established for polymer lattices cannot be transferred directly to metal lattices produced by ADAM. The constraints of bound-metal extrusion — the overhang limitations inherited from fused deposition modelling, the support architecture required to bridge cellular interiors, and the dimensional evolution during sintering — render a substantial fraction of the topologies of interest either non-manufacturable or non-testable. The economic and temporal burden of the multi-stage ADAM workflow is, in addition, incompatible with the full-factorial experimental design of the size employed for the polymer specimens. A structured follow-up study, centred on a direct ADAM-versus-SLM comparison on a common 17-4 PH feedstock, on a reduced Taguchi L18 orthogonal array, and on the same statistical pipeline developed for the polymer specimens, is therefore proposed as the natural continuation of the metallic part of the work. The recommended pipeline retains the diagnostic suite, the Box–Cox transformation and the Prediction-Profiler-based desirability optimisation of the polymer study, so that the polymer and metal data sets remain directly comparable at every level of the statistical analysis.

9 CONTRIBUTIONS OF THE WORK

9.1 Contributions to theory

The dissertation extends the theoretical understanding of the interaction between lattice topology, cell size and the manufacturing process in additive manufacturing. Its principal theoretical contribution is the quantitative, statistically founded demonstration that the mechanical response of additively manufactured polymer lattices is governed jointly by the topology of the unit cell and by the consolidation route of the manufacturing process, and that the cell size, within a constant-density regime, plays only a secondary role. The Structure × Materials interaction identified by the least-squares analysis provides a transparent quantitative measure of the process–structure coupling and explains, on a physically defensible basis, why the relative advantage of laser SLS over MJF grows with the geometric demand placed on the process by the lattice topology.

A second theoretical contribution is the introduction of the volume-specific force $f = F / V$ as a complementary descriptor of the lattice response. The volumetric force removes the dependence on the bounding cross-section of the lattice specimen and provides a topology-independent and size-independent basis for the comparison of lattices that differ in their internal architecture and in their consolidated mass. It is the natural mass-efficiency descriptor for lightweight engineering applications and, when reported alongside the conventional peak force, substantially strengthens the cross-topology comparability of the experimental data.

A third theoretical contribution is the development of an integrated statistical evaluation framework that combines the design of experiments, classical ANOVA, least-squares modelling, diagnostic residual analysis, Box–Cox transformation and Prediction-Profiler-based desirability optimisation. The framework was applied to all responses examined in the dissertation and provides a transparent, reproducible basis for the parametric description of the lattice response. It is sufficiently general to be transferred to other materials, topologies and manufacturing technologies, and represents a methodological contribution to the broader field of statistically founded additive manufacturing research.

9.2 Contributions to practice

From the standpoint of practical applicability, the dissertation provides engineering recommendations for the selection of lattice–process combinations as a function of the design objective. For applications requiring the highest initial stiffness, the optimal combination is the Gyroid topology at a 9 mm cell produced by MJF on the HP platform. For applications requiring the highest strength at the first stress maximum and the highest energy absorption, the recommended combination is the Gyroid topology at a 9 mm cell produced by laser SLS on the EOS platform. The BCC strut topology is identified as the appropriate choice when a low initial stiffness and a progressive, ductile collapse without sudden failure are desired — for example as a compliant core in sandwich structures, as an energy-dissipating interface, or for medical applications aiming to mimic the compliance of cancellous bone tissue.

A further practical contribution is the explicit delimitation of the manufacturing envelope of ADAM for cellular geometries in 17-4 PH stainless steel. The dissertation establishes that ADAM is a viable route for simple, support-tolerant strut-based geometries oriented for minimum overhang, and an unsuitable route for the TPMS topologies that offer the highest specific mechanical performance. The empirical evidence is supported by an inspection of the build preparation in the Markforged Eiger slicer, which shows that the limitation of ADAM for three-dimensional lattices is not solely a property of the physical deposition process but is jointly imposed by the deposition physics and by the assumptions hard-coded into the build-preparation environment available for the platform.

Based on the metallic feasibility campaign, the dissertation outlines a structured follow-up study centred on a direct ADAM-versus-SLM comparison on a common 17-4 PH feedstock, on a reduced Taguchi L18 orthogonal array, and on the same statistical pipeline developed for the polymer specimens. The proposed study would deliver the statistically conclusive characterisation of metal cellular performance that the present feasibility campaign has not been able to provide and would do so at a specimen count that is compatible with the cost structure of metal additive manufacturing.

The presented results are directly applicable in the aerospace, automotive, biomedical and protective-equipment sectors, where the simultaneous optimisation of mass, stiffness, strength and energy-absorption capacity constitutes a primary engineering objective. The statistical methodology developed in the work can be adopted by industrial research and development departments seeking to optimise additive manufacturing parameters under explicit budgetary and temporal constraints.

CONCLUSION

The presented dissertation has addressed the experimental and statistical investigation of additively manufactured polymer and metal lattice structures, with a focus on the influence of the unit-cell topology, the cell size and the manufacturing process on the macroscopic compressive response of the printed specimens. The aim of the work was to identify the factors that govern the mechanical response of the lattices, to develop a transparent statistical framework for their quantitative comparison, and to delimit the manufacturing envelope within which the investigated processes can usefully contribute to the production of cellular components.

The polymer campaign compared the body-centred-cubic (BCC) strut topology with the Gyroid and Schwarz Diamond TPMS topologies at three cell sizes and on two powder-bed fusion platforms — Selective Laser Sintering on the EOS Formiga P 110 Velocis with white PA 12 (EOS PA 2200) and Multi Jet Fusion on the HP Jet Fusion 5200 with dark PA 12 (HP 3D High Reusability PA 12). The experimental data were processed by analysis of variance in Minitab 17 and by least-squares modelling in JMP, with diagnostic residual analysis, Box–Cox transformation and Prediction-Profiler-based desirability optimisation. The statistical evaluation identified the Materials factor (consolidation route) and the Structure factor (unit-cell topology) as the dominant influences on the peak compressive force and on the volume-specific force f, together with a strong Structure × Materials interaction that quantifies the process–structure coupling on a physically defensible basis. The cell size emerged as statistically not significant within the explored 6 – 9 mm range, at constant solidity.

The metallic campaign investigated the feasibility of producing geometrically equivalent lattice structures by Atomic Diffusion Additive Manufacturing on the Markforged Metal X system with 17-4 PH precipitation-hardenable stainless steel. The campaign demonstrated that the geometric and statistical conclusions established for polymer lattices cannot be transferred directly to ADAM. The constraints of bound-metal extrusion — the overhang limitations inherited from fused deposition modelling, the support architecture required to bridge cellular interiors, and the dimensional evolution during sintering — render a substantial fraction of the topologies of interest either non-manufacturable or non-testable. Simple, support-tolerant strut topologies oriented for minimum overhang are reliably producible; TPMS topologies, by contrast, yield essentially no specimens of testable quality, regardless of the orientation explored.

Based on these findings, a structured follow-up study has been outlined as the natural continuation of the metallic part of the work. The proposed study is centred on a direct ADAM-versus-SLM comparison on a common 17-4 PH feedstock, adopts a Taguchi L18 orthogonal array in place of the polymer study's full factorial in order to reduce the specimen count to a level compatible with the cost structure of metal additive manufacturing, conducts compression testing according to ISO 13314, and analyses the resulting data through the same statistical pipeline developed for the polymer specimens. Within the limits of the present investigation, the work establishes that ADAM is a viable manufacturing route for simple, support-tolerant cellular geometries in 17-4 PH stainless steel, an unsuitable route for the geometrically demanding lattice topologies that offer the highest specific mechanical performance, and a process whose application envelope is best characterised through the structured comparison with SLM outlined above.

The dissertation contributes to the current understanding of additive manufacturing on three principal levels. On the theoretical level, it provides a quantitative, statistically founded demonstration of the joint influence of topology, material and manufacturing process on the mechanical response of additively manufactured polymer lattices, introduces the volume-specific force f as a complementary mass-efficiency descriptor, and develops an integrated statistical evaluation framework that is transferable to other materials, topologies and manufacturing technologies. On the practical level, it provides engineering recommendations for the selection of lattice–process combinations, delimits the manufacturing envelope of ADAM for cellular geometries in 17-4 PH stainless steel, and outlines a structured follow-up study for the metallic part of the research. On the methodological level, it demonstrates that the choice of structure type and of manufacturing route exerts a decisive influence on the monitored mechanical responses, with their mutual interaction being critical for the attainment of an optimal lattice configuration, and that the cell size can be selected on the basis of secondary design criteria without an appreciable penalty on the macroscopic response provided that the minimum-cell-count requirement of ISO 13314 is respected.

RESUMÉ

Dizertačná práca sa zaoberá experimentálnym hodnotením vplyvu topológie elementárnej bunky, jej veľkosti a zvolenej výrobnej technológie na mechanickú odozvu mriežkových štruktúr vyrábaných aditívnymi technológiami. Práca pokrýva polymérne aj kovové vstupné materiály a explicitne sa venuje rozhraniu medzi týmito dvomi materiálovými skupinami tým, že výrobnú technológiu rovnocenne zaraďuje medzi sledované faktory popri topológii a veľkosti bunky.

V polymérnej časti boli porovnané tri topológie mriežkových štruktúr — telesovo centrovaná kubická topológia (BCC) a topológie trojito periodických minimálnych plôch Gyroid a Schwarz Diamond — pri troch veľkostiach buniek (6, 7,5 a 9 mm) a na dvoch zariadeniach fúzie v práškovom lôžku: selektívneho laserového spekania (SLS) na zariadení EOS Formiga P 110 Velocis s bielym PA 12 (EOS PA 2200) a technológie Multi Jet Fusion (MJF) na zariadení HP Jet Fusion 5200 s tmavým PA 12 (HP 3D High Reusability PA 12). Vzorky boli vyrobené v súlade s normou ISO 13314 a podrobené kvázistatickej tlakovej skúške na univerzálnom skúšobnom stroji Zwick/Roell Z150.

Experimentálne údaje boli spracované dvojstupňovou štatistickou analýzou. V prvom kroku bola realizovaná analýza rozptylu (ANOVA) v softvéri Minitab 17 pre štyri sledované odpovede — kvázielastický gradient EC, prvé maximum napätia σ_{peak}, plošinové napätie σ_{pl} a hustotu absorbovanej energie W. V druhom kroku boli rovnaké údaje spracované metódou najmenších štvorcov v softvéri JMP, vrátane diagnostickej analýzy reziduí, Box–Coxovej transformácie a optimalizácie pomocou funkcie želateľnosti v module Prediction Profiler. Súčasťou analýzy bolo aj zavedenie objemovo špecifickej sily f = F / V ako komplementárneho deskriptora odozvy mriežkových štruktúr, ktorý vzťahuje nameranú silu na menovitý CAD objem vzorky a umožňuje porovnávať štruktúry s rôznou vnútornou architektúrou bez závislosti od ich vonkajšieho prierezu.

Štatistická analýza identifikovala materiál (cestu konsolidácie) a topológiu elementárnej bunky ako dominantné faktory ovplyvňujúce mechanickú odozvu polymérnych mriežkových štruktúr. Silná interakcia Štruktúra × Materiál preukázala, že relatívna výhoda laserového spekania (SLS) voči technológii MJF rastie s geometrickou náročnosťou topológie — najvýraznejšie pri štruktúre Schwarz Diamond, kde rozdiel medzi kombináciami S–W a S–B dosahuje až trojnásobok nameranej sily. Faktor veľkosti bunky sa v skúmanom intervale 6 – 9 mm pri konštantnej hustote výplne (solidity 0,2) ukázal ako štatisticky nevýznamný, čo znamená, že veľkosť bunky možno voliť podľa sekundárnych konštrukčných kritérií bez výrazného vplyvu na makroskopickú odozvu.

V kovovej časti práce bola experimentálne overovaná možnosť výroby ekvivalentných mriežkových štruktúr technológiou Atomic Diffusion Additive Manufacturing (ADAM) na zariadení Markforged Metal X z precipitačne vytvrdzovanej nehrdzavejúcej ocele 17-4 PH. Kampaň preukázala, že geometrické závery získané pri polymérnych vzorkách nemožno priamo prenášať na ADAM. Obmedzenia procesu vyplývajúce z extrúzie kovom plneného polymérneho filamentu — najmä nutnosť podporných štruktúr pri previsoch a vnútorných premosteniach — spôsobujú, že významná časť topológií je buď nevyrobiteľná, alebo nevhodná na následné mechanické testovanie. Jednoduché podpierateľné štruktúry sú spoľahlivo vyrobiteľné, kým topológie typu TPMS prakticky neumožňujú dosiahnuť funkčné vzorky.

Na základe zistení bol navrhnutý štruktúrovaný nadväzujúci výskum, ktorý porovná technológie ADAM a Selective Laser Melting (SLM) na spoločnom materiáli 17-4 PH s využitím Taguchiho ortogonálneho poľa L18 a rovnakého štatistického vyhodnocovacieho postupu, aký bol vyvinutý v polymérnej časti. Týmto sa zabezpečí priama porovnateľnosť polymérnej a kovovej kampane na všetkých úrovniach štatistickej analýzy.

Z teoretického hľadiska práca prispieva ku kvantitatívnemu pochopeniu interakcie medzi topológiou, materiálom a výrobnou technológiou pri aditívnej výrobe mriežkových štruktúr, zavádza objemovo špecifickú silu ako mierku hmotnostnej efektivity a vytvára prenosný štatistický rámec pre vyhodnocovanie podobných experimentov. Z praktického hľadiska poskytuje odporúčania pre výber kombinácie topológie a výrobnej technológie pre aplikácie v leteckom, automobilovom, biomedicínskom a ochrannom priemysle a zároveň jasne vymedzuje aplikačný rozsah technológie ADAM pri výrobe kovových mriežkových štruktúr.

Výber zoznamu použitej literatúry

GIBSON, I., ROSEN, D. W., STUCKER, B. Additive Manufacturing Technologies: Rapid Prototyping to Direct Digital Manufacturing. New York: Springer, 2010.

GAO, W. et al. Additive Manufacturing: Current State, Future Potential, Gaps and Needs, and Recommendations. 2015.

WOHLERS, T., GORNET, T. 3D Printing and Additive Manufacturing: Principles and Applications. New York: Springer, 2014.

SCHMID, M. Selektives Lasersintern (SLS) mit Kunststoffen. München: Hanser, 2018.

RIEDELBAUCH, J., RIETZEL, D., WITT, G. Analysis of material aging and the influence on the mechanical properties of polyamide 12 in Multi Jet Fusion. Additive Manufacturing, 2019.

ROSSO, S., Meneghello, R., BIASETTO, L., GRIGOLATO, L., CONCHERI, G., SAVIO, G. In-depth comparison of polyamide 12 parts manufactured by Multi Jet Fusion and Selective Laser Sintering. Additive Manufacturing, 2020.

XU, Z., WANG, Y., WU, D., ANANTH, K. P., ZHAO, J. Process and performance evaluation of the Selective Laser Sintering and Multi Jet Fusion processes. Additive Manufacturing, 2019.

LUPONE, F., PADOVANO, E., CASAMENTO, F., BADINI, C. Process Phenomena and Material Properties in Selective Laser Sintering of Polymers: A Review. Materials, 2024.

HABIB, F. N., IOVENITTI, P., MASOOD, S. H., NIKZAD, M. Fabrication of polymeric lattice structures for optimum energy absorption using Multi Jet Fusion technology. Materials & Design, 2018.

HAN, X. et al. A Review of the Multi Jet Fusion Process. Polymers, 2022.

MARKFORGED. Metal X System Technical Specifications. Watertown: Markforged, 2020.

MARKFORGED. Metal Materials for the Metal X System. Watertown: Markforged, 2024.

PARENTI, P. et al. On the relationship between process parameters and part quality in Atomic Diffusion Additive Manufacturing. International Journal of Advanced Manufacturing Technology, 2022.

MOSTAFAEI, A. et al. Binder jet 3D printing — Process parameters, materials, properties and challenges. Progress in Materials Science, 2020.

ISO 13314:2011. Mechanical testing of metals — Ductility testing — Compression test for porous and cellular metals. Geneva: International Organization for Standardization, 2011.

ISO/ASTM 52900:2021. Additive manufacturing — General principles — Fundamentals and vocabulary. Geneva: ISO, 2021.

BERNARD, A. R., ELSAYED, M. S. A. Design, Manufacturing, and Analysis of Periodic Three-Dimensional Cellular Materials for Energy Absorption Applications: A Critical Review. Materials, 2024.

AHMAD, A., BELLUOMO, L., BICI, M., CAMPANA, F. Bird's Eye View on Lattice Structures: Design Issues and Applications for Best Practices in Mechanical Design. Metals, 2023.

COLOSIMO, B. M., GRASSO, M., GARGHETTI, F., ROSSI, B. Complex geometries in additive manufacturing: A new solution for lattice structure modelling and monitoring. Quality Engineering, 2022.

Kompletný zoznam použitej literatúry de k dispozícii v dizertačnej práci

Zoznam publikačnej činnosti

KRIŠÁK, D., STANISLAV, J., PETRŮ, J., ČEP, R., MATUŠ, M., CZÁN, A., CZÁNOVÁ, N. Degradation of PA12 Powder from SLS Technology. Cham: Springer, 2026, vol. 1667, pp. 287 – 297. DOI: 10.1007/978-3-032-07721-9_26.

CZÁN, A., CZÁNOVÁ, N., HOLUBJÁK, J., CZÁNOVÁ, T., **KRIŠÁK, D.**, MARKOVIČ, M. Comparison of Selective Laser Melting and Atomic Diffusion Additive Manufacturing Technologies: Evaluating Stainless Steel Materials in Terms of Accuracy and Key Performance Indicators. Procedia CIRP, 2026, vol. 93, pp. 502 – 509. DOI: 10.1016/j.trpro.2025.11.077. Indexed in Web of Science Core Collection (ESCI) and Scopus.

MIZERA, O., CEPOVÁ, L., ZELINKA, J., JEŽEK, D., MALANT, J., KRYSKA, D., **KRIŠÁK, D.**, TKÁČ, J. Influence of the Measurement of Anti-Reflective Coating Layer for Optical Measurement. MM Science Journal, 2025, September, pp. 8504 – 8511. ISSN 1805-0476. DOI: 10.17973/MMSJ.2025_09_2025084.

CZÁN, A., CZÁNOVÁ, T., HOLUBJÁK, J., NOVÁK, M., CZÁN, A., CZÁNOVÁ, N., **KRIŠÁK, D.** Analysis of the Basic Characteristics of the Working Accuracy of the Atomic Diffusion Additive Manufacturing ADAM Process by Comparison with the Selective Laser Melting SLM Process. Manufacturing Technology, 2024, vol. 24, no. 1, pp. 15 – 27. ISSN 1213-2489. DOI: 10.21062/mft.2024.015.

CZÁN, A., CZÁNOVÁ, N., KURIC, I., CZÁNOVÁ, T., HOLUBJÁK, J., CZÁN, A., **KRIŠÁK, D.** Selective Laser Sintering vs. Multi Jet Fusion as a Basic Comparative Study of PA12 Polyamide Based on Accuracy and Significant Indicators. In: RYSIŃSKI, J., WIĘCEK, D., eds. Production Engineering and Management. Bielsko-Biała: Wydawnictwo Naukowe Uniwersytetu Bielsko-Bialskiego, 2024. ISBN 978-83-67652-27-8. DOI: 10.53052/9788367652278.

BECHNÝ, V., MATUŠ, M., JOCH, R., DRBÚL, M., CZÁN, A., CEDZO, M., **KRIŠÁK, D.** The Influence of Orientation by SLM Additive Manufacturing Process on Surface Integrity. Cham: Springer, 2024, pp. 206 – 215. DOI: 10.1007/978-3-031-65656-9_21.

MATUŠ, M., BECHNÝ, V., ŠAJGALÍK, M., MARKOVIČ, J., DRBÚL, M., CEDZO, M., JOCH, R., **KRIŠÁK, D.** Implementation of Advanced Techniques for Quality Assessment of Metal Parts Produced by SLM Technology. Cham: Springer, 2024, pp. 78 – 88. DOI: 10.1007/978-3-031-65656-9_8.

MECHALI, A., MESÍČEK, J., MA, Q.-P., HAJNYS, J., GAUTAM, P., BLAHA, R., **KRIŠÁK, D.**, PETRŮ, J. Abrasive Surface Treatment of AlSi10Mg Parts Made by L-PBF. MM Science Journal, 2024, no. 1. ISSN 1803-1269. DOI: 10.17973/MMSJ.2024_02_2023134.

PECIAR, P., FEKETE, R., PECIAROVÁ, M., KRUCAY, P., MESÍČEK, J., **KRIŠÁK, D.**, PECIAR, M. Modification of Powder Material for 3D Printing Using Dry Granulation. MM Science Journal, 2024, no. 4. ISSN 1803-1269. DOI: 10.17973/MMSJ.2024_10_2024067.

MECHALI, A., HLINKA, J., MESÍČEK, J., HAJNYS, J., ZELINKA, J., **KRIŠÁK, D.**, CEPOVÁ, L., BLAHA, R., ČEP, R., PETRŮ, J. Effect of Tumbling on the M300 Maraging Steel Parts Made by Selective Laser Melting. MM Science Journal, 2024, no. 4. ISSN 1803-1269. DOI: 10.17973/MMSJ.2024_10_2024068.

BLAHA, R., HAJNYS, J., MESÍČEK, J., MECHALI, A., **KRIŠÁK, D.**, PAGÁČ, M. Review of Directed Energy Deposition (DED) in Component Repair. Cham: Springer, 2024, pp. 197 – 205. DOI: 10.1007/978-3-031-65656-9_20.

CZÁN, A., CZÁNOVÁ, T., HOLUBJÁK, J., NOVÁK, M., CZÁN, A., CZÁNOVÁ, N., **KRIŠÁK, D.** Comparative Evaluation of Working Accuracy in the Atomic Diffusion Additive Manufacturing (ADAM) Process and the Binder Jetting (BJ) Process by Analysing Key Characteristics. Manufacturing Technology, 2023, vol. 23, no. 6, pp. 769 – 780. ISSN 1213-2489. DOI: 10.21062/MFT.2023.108. Indexed in Web of Science Core Collection (ESCI) and Scopus.

BLAHA, R., **KRIŠÁK, D.**, HAJNYS, J., MESÍČEK, J., PAGÁČ, M., JANČAR, L., JANSA, J., POSMYKOVÁ, E., GAZDA, M. Experimental Verification of Process Parameters Influencing the Mechanical Properties of M300 in the SLM Process. MM Science Journal, 2023, no. 2. ISSN 1803-1269. DOI: 10.17973/MMSJ.2023_06_2023038.